International Journal of Adhesion & Adhesives 143 (2025) 104162

Contents lists available at ScienceDirect

International Journal of Adhesion and Adhesives

journal homepage: www.elsevier.com/locate/ijadhadh

A multifunctional dendrimer for BPA-free dental adhesives: Polymerization behavior and cytotoxic profile of G-IEMA

Diogo Monteiro [a], Margot Barbier [a], António HS Delgado [a,*], Luísa Gonçalves [a], Miguel Chaves-Ferreira [b], Joana Vasconcelos e Cruz [a], Mário Polido [a]

[a] Egas Moniz Interdisciplinary Research Center (CiiEM), Egas Moniz School of Health & Science, Campus Universitário, Quinta da Granja, Monte de Caparica, 2829-511, Almada, PT, Portuguese Republic

[b] iNova4Health, NOVA Medical School, Universidade Nova de Lisboa, Campo Mártires da Pátria 130, Lisboa, 1169-056, Portuguese Republic

ARTICLE INFO

Keywords:
Dendrimer
G-IEMA
Universal adhesive
Polymerization kinetics
Cytotoxicity
Bis-GMA substitute

ABSTRACT

To determine whether substituting Bis-GMA for dendritic macromer G-IEMA in a universal adhesive alters real-time cure/post-cure performance and in-vitro cytotoxicity. Polymerization kinetics of five neat monomers (Bis-GMA, G-IEMA, UDMA, TEGDMA, HEMA) and four adhesives, two commercial controls (Scotchbond Universal, Futurabond M+) and two experimental formulations differing only in the base monomer, EXP-BIS vs. EXP-G, with 25 wt% of Bis-GMA or G-IEMA, respectively, were monitored by real-time ATR-FTIR for 20 min cure/post-cure ($n = 3$). Key outputs were final degree of conversion (DC_{max}), maximum polymerization rate (Rp_{max}) and half-time ($t_{0.5}$). Cytocompatibility was assessed on primary human dental-pulp cells via 24 h MTT and propidium-iodide (PI) assays using extracts of polymerized and non-polymerized specimens ($n = 12$). Among homopolymers, DC_{max} did not differ (one-way ANOVA, $p = 0.24$) while $R_{p,max}$ did ($p < 0.0001$), with G-IEMA and TEGDMA faster than Bis-GMA; $t_{0.5}$ was similar ($p = 0.15$). Across adhesives, DC_{max} ($p = 0.06$), Rp_{max} ($p = 0.89$) and $t_{0.5}$ ($p = 0.27$) were comparable; EXP-GI reached the highest DC_{max} (≈89 %). G-IEMA was less cytotoxic than Bis-GMA in both assays: MTT +20 % and +51 % in non-polymerized and polymerized extracts, respectively; PI −40 % and −54 % (all pairwise $p < 0.01$). For adhesive extracts, MTT showed a main effect of adhesive (two-way ANOVA, $p < 0.001$) but no treatment effect/interaction; relative to Scotchbond, EXP-GI supported +6.7 % (non-polymerized) and +18.2 % higher metabolic activity, while all adhesives remained below the control ($p < 0.001$). After polymerization, EXP-GI exhibited 17 % lower apoptosis than Scotchbond ($p = 0.049$) and 11 % lower than Futurabond ($p < 0.05$). G-IEMA can replace Bis-GMA without compromising cure efficiency or increasing acute cytotoxicity, supporting its use in BPA-free universal adhesives.

1. Introduction

Universal (multimode) dental adhesives have transformed chair-side protocols by enabling reliable and versatile bonding to enamel, dentin, resin composite, metal alloys and ceramic substrates with a single bottle [1,2]. Their clinical versatility, however, relies on a delicate compromise between self-etching efficacy, hydrophilic and hydrophobic component mixtures and long-term hydrolytic stability. For this reason, several universal adhesive formulations currently exist in the dental market [3]. Classical universal adhesives are blends of dimethacrylate monomers and amphiphilic co-monomers (often 2-hydroxyethyl methacrylates [HEMA]) dissolved in a solvent, photoinitiators and dispersed in small silica nanoparticles or glass fillers [2]; their "universal" character derives from functional acidic monomers, most commonly 10-methacryloyloxydecyl dihydrogen phosphate (10-MDP), that promote chemical interaction with hydroxyapatite and oxide ceramics, while some systems (e.g., Scotchbond Universal) also include a polyalkenoic acid copolymer and/or silane to extend substrate compatibility [4]. The presence and balance of these components (pH range of ≈2–3, solvent type, HEMA content) govern phase stability, water sorption and durability [5,6], with type of functional monomer determining stable Ca-MDP salt formation [7,8] and potential interfacial nano-layering at dentine [8,9].

Most commercial adhesive systems still center on bisphenol-A-glycidyl dimethacrylate (Bis-GMA) because of its decent physical properties, high molecular weight and low polymerization shrinkage

* Corredponding author.
E-mail address: asalesdelgado@egasmoniz.edu.pt (A.H. Delgado).

https://doi.org/10.1016/j.ijadhadh.2025.104162
Received 5 August 2025; Received in revised form 17 September 2025; Accepted 18 September 2025
Available online 23 September 2025

[10]. Recent market audits show >70 % of resin-based dental materials contain BPA derivatives, many used in paediatric indications. Yet Bis-GMA is intrinsically viscous, limits overall double-bond conversion and its degradation byproducts include trace bisphenol-A (BPA), an endocrine disruptor [11,12]. In vitro work shows Bis-GMA generates markedly more reactive oxygen species and DNA double-strand breaks than other common co-monomers [13]; Compounding the toxicological findings, the European Food Safety Authority has cut the tolerable daily intake of BPA by 20 000-fold (to 0.2 ng kg^{-1} day^{-1}) and the EU will bar BPA from food-contact materials in 2025 [14], underscoring regulators' shift toward a no-safe-level stance for endocrine disruptors. Because Bis-GMA and its hydrolysis product BPA display non-monotonic dose–response behaviour, where even picomolar exposure can trigger estrogenic or immunomodulatory pathways, simply lowering residual monomer content may be insufficient [15]. These biochemical and regulatory pressures intensify the demand for BPA-free, highly cross-linkable macromers that can achieve high double-bond conversion without biological or legislative liabilities.

In response, emerging Bis-GMA substitutes span (i) bio-based di(meth)acrylates (e.g., isosorbide-derived IBM/ISDMMA; guaiacol/creosol-derived dimethacrylates) that report high conversion, lower estrogenic activity and improved hydrolytic resistance, and (ii) architectural approaches (hyperbranched/dendritic macromers) aimed at raising functionality while controlling viscosity and leaching. Dendritic methacrylates such as G(2)-isocyanatoethyl methacrylate (G-IEMA) may provide a compelling, BPA-free alternative. A star-burst architecture lowers viscosity, enhances monomer mobility and presents eight terminal methacrylate groups capable of forming highly cross-linked, aromatic-free networks [16]. Early mechanical screens already reported higher degree of conversion (DC), reduced shrinkage stress and greater fracture toughness when Bis-GMA was replaced by G-IEMA [4]. In 2019, our group first included G-IEMA in an experimental adhesive and demonstrated dentin microtensile bond strength and mechanistic properties equivalent to Scotchbond Universal (3M ESPE, USA) and Futurabond M+ (VOCO, Germany) controls [17]. Further to this, SEM mapping [18] confirmed well-adapted hybrid layers and stable bond strength after 24 h water storage across etch-and-rinse and self-etch modes of the experimental adhesives, and later in 2022 [19], it was possible to observe that G-IEMA lowered nanoleakage and preserved bond strength after thermocycling, indicating acceptable hydrolytic resilience. This prior work with G-IEMA dendrimer established promising bond performance and micro-morphology interaction but did not resolve whether any kinetic advantage exists *in situ* nor whether such differences map onto short-term pulp-cell cytocompatibility. Yet translation remains limited because most studies characterise either mechanics or cytocompatibility in isolation; very few interrogate real-time cure kinetics and acute biological response within the same chemical system, particularly for dendritic methacrylates used in universal adhesive.

To close this gap, we coupled real-time ATR-FTIR polymerization kinetics on neat monomers and matched universal-adhesive matrices with biological outcomes (24 h MTT and PI flow cytometry) from primary human dental-pulp cells, comparing a G-IEMA-based experimental adhesive (EXP-GI) directly with its Bis-GMA analogue (EXP-BIS) and two market references for benchmark. Testing the neat monomers in parallel isolates intrinsic toxicity from network-driven leaching and allows attribution of any adhesive-level effects to base-monomer chemistry rather than confounders (solvent, initiator, functional monomer). This integrated design provides missing mechanistic evidence on whether a dendritic, BPA-free macromer can match clinical cure performance while improving cytocompatibility, thereby informing the translational relevance of dendritic monomers alongside other leading Bis-GMA alternatives now reported in the literature. The null hypotheses were that replacing Bis-GMA with G-IEMA would produce no statistically significant differences in (i) polymerization kinetic parameters or (ii) cytotoxicity.

2. Experimental

2.1. Materials

Industrial-grade methacrylate monomers—10-MDP, Bis-GMA, G-IEMA, UDMA, TEGDMA, and HEMA—were used as received; chemical structures are shown in Fig. 1; suppliers and properties are summarized in Table 1. The synthesis of G-IEMA is given in previously published publications and is addressed in Table 1. Camphorquinone (CQ) and ethyl-4-dimethylaminobenzoate (EDAB/BDA) were used as the photoinitiator system. Two experimental adhesives were considered: EXP-BIS (Bis-GMA-based) and EXP-GI (Bis-GMA fraction replaced by G-IEMA). Scotchbond Universal (3M ESPE, St. Louis, USA) and Futurabond M+ (VOCO, Cuxhaven, Germany) served as commercial benchmarks.

2.2. Homopolymer and experimental adhesive formulations

Each neat monomer formulation contained 98.8 mol% monomer, 0.4 mol% CQ, and 0.8 mol% BDA, mixed for 24 h at room temperature with magnetic stirring. Bis-GMA blends were briefly warmed to 50 ± 2 °C to aid initiator dissolution. Mixtures were protected from ambient light, refrigerated for 24 h at 2 °C, and equilibrated to 22 ± 2 °C for 2 h before testing. EXP-BIS was prepared according to the wt% given in Table 2; in EXP-GI, the Bis-GMA fraction (25 wt% of the formulation) was replaced 1:1 by G-IEMA, with all other components unchanged. Homopolymer films (3 μL) were light-cured directly on an ATR diamond (950 mW/cm^2, 40 s). Adhesive discs (5 mm × 0.5 mm) were molded in PTFE and cured identically. This concentration was chosen since it mimics typical ranges of Bis-GMA found in commercial adhesives. No inorganic fillers were added to isolate monomeric effects.

2.3. Polymerization kinetics (ATR-FTIR)

For every formulation, 3 μL aliquots were dispensed with a calibrated micropipette (SuperfleX™, Sigma-Aldrich, Burlington, MA, USA) directly onto the ATR diamond and confined within a metal ring (Ø 10 mm × 1 mm; volume ≈ 0.08 cm^3). This produced a clinically relevant, ultrathin film that covered only the crystal. Specimens were solvent-flashed for 20 ± 5 s with a 1600 W hair-dryer positioned 15 cm away (Calor CV5312C0, Ecully, France). Polymerization was initiated with an LED curing unit (Elipar Deep Cure-S, 3M ESPE, USA) held in contact to an acetate sheet barrier, at zero distance from the samples. Irradiance, verified every third use with an Optilux radiometer (Kerr, Orange, CA, USA), remained at a minimum of 900 ± 150 mW/cm^2 across a 430–480 nm emission band. Curing commenced 20 ± 5 s after specimen placement for neat monomers and 40 ± 10 s for adhesives (additional drying step) and lasted for 15 s.

Real-time ATR-FTIR spectra (700–4000 cm^{-1}, 4 cm^{-1} resolution) were collected at 22 ± 2 °C starting 20 s before light-curing and lasting continuously for 20 min (n = 3 replications per material), originating 677 scans for each run. Acetone was used to clean the ATR crystal between runs. Data were processed using Spectrum TimeBase v3.1.4 (Perkin-Elmer) and DC_{max} was derived following Delgado et al. (2021) [20]:

In order to calculate the degree of conversion at time t, the following equation (1) was used,

$$D_C\,(\%) = \left[1 - \left(\frac{A_t}{A_0}\right)\right] * 100 \quad (1)$$

(1) where A_0 and A_t are the C-O stretch absorbance at 1320 cm^{-1} above background level at 1345 cm^{-1} initially and at time t after start of polymerization. Using the 1320 cm^{-1} band—rather than the traditional 1640 cm^{-1} C=C peak—avoids systematic errors previously detailed (see *Ref.* [20]). The 1585 cm^{-1} region overlaps aromatic/amine/amide modes and is perturbed by urethane amide II and the CQ/BDA tertiary

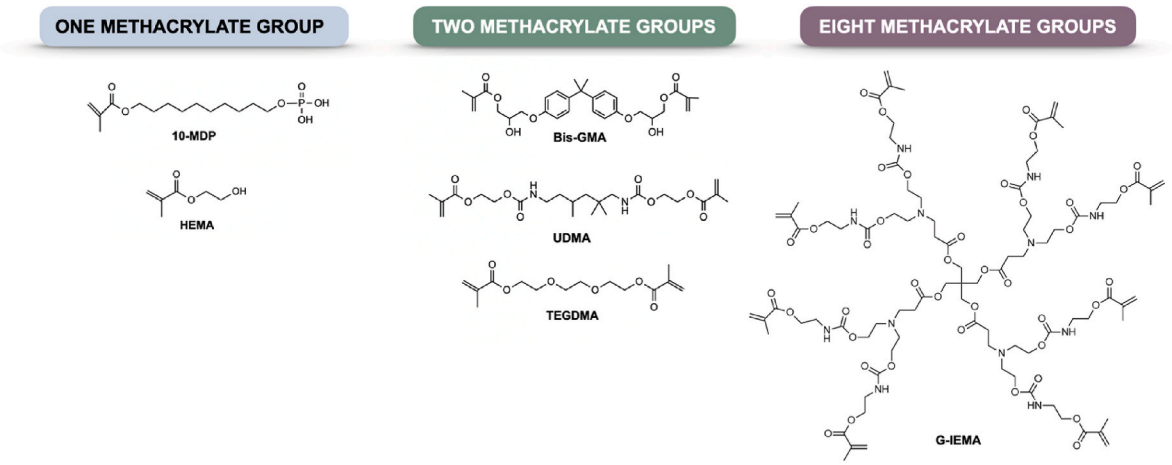

Fig. 1. Chemical structure of monomethacrylates (10-MDP and HEMA), dimethacrylates (Bis-GMA, UDMA and TEGDMA) and G-IEMA, containing 8 methacrylate groups in its dendrimer branches.

amine, so it is not invariant during cure. Also, the 1715–1730 cm^{-1} carbonyl band is often used as a reference peak, but in the solvent-rich HEMA/MDP matrices it splits into a shifting free/H-bonded doublet that changes with solvent loss, hydrogen-bonding, and network formation—violating the requirement for a cure-independent reference. Continuous acquisition without removing the sample from the crystal, in our method, eliminated the need for an internal reference peak.

From the DC–time curve, DC_{max} and kinetic parameters were extracted:

- Maximum polymerization rate (Rp_{max}, % s^{-1}) — first derivative peak of DC(%)/time.
- Half-time ($t_{0.5}$, s) — time to reach 50 % of DC_{max}.

These metrics quantify both the extent and speed of cure under conditions that closely emulate clinical film thickness and light exposure.

2.4. Test materials and extract preparation

Uncured adhesives and neat monomers were first dissolved in absolute ethanol to 250 mg mL^{-1}. Aliquots of each stock were then diluted with Dulbecco's Modified Eagle's Medium (DMEM, Sigma-Aldrich, St. Gallen, Switzerland) to a working concentration of 0.125 mg mL^{-1}. To mimic the relative proportions present in the experimental and commercial adhesives, additional serial dilutions of the monomer extracts were prepared to the maximum percentage each monomer contributes to an adhesive formulation: G-IEMA 15 %, Bis-GMA 25 %, HEMA 25 %, TEGDMA 10 %, and UDMA 10 % (w/v, referenced to the 0.125 mg mL^{-1} stock).

For polymerized extracts, 100 μL of each adhesive or neat monomer was dispensed onto a sterile silicone pad and light-cured for 40 s with an Elipar Deep Cure-S LED unit (3M ESPE, USA; 1470 mW/cm^2, 430–480 nm). Each cured disc was transferred aseptically into a 15 mL polypropylene tube containing 5 mL of DMEM and incubated at 37 °C for 24 h (5 % CO_2, Sanyo MCO-18AIC). The resulting eluates, polymerized and non-polymerized, were filtered (0.22 μm) and used immediately.

2.5. Cell culture

Primary human dental-pulp cells previously established in our laboratory [21] were revived from liquid-nitrogen stock (passage ≤3, frozen at ≈ 90 % confluence). Cells were thawed into DMEM supplemented with gentamicin (50 μg mL^{-1}) and amphotericin B (2.5 μg mL^{-1}), gently resuspended, and centrifuged (5 min, 1500 rpm, Heraeus Megafuge 1.0/1.0R). The pellet was re-suspended in antibiotic-free DMEM and seeded into T-25 flasks. Cultures were maintained at 37 °C, 5 % CO_2 until 90–95 % confluence, washed with PBS, and detached with trypsin-EDTA. Cell density was determined by trypan-blue exclusion, then plated into 96-well plates at 1×10^4 cells $well^{-1}$ (100 μL) and allowed to adhere overnight before exposure to extracts.

2.6. MTT metabolic-activity assay

At 90–95 % confluence, growth medium was replaced with 100 μL of each test extract (adhesive, monomer, or control medium) and plates were incubated for 24 h. Wells were then rinsed with 100 μL PBS, followed by 100 μL of MTT working solution (0.5 mg mL^{-1}; 1:9 dilution of 5 mg mL^{-1} stock in sterile PBS with DMEM). After 3 h at 37 °C, 150 μL isopropanol was added to solubilize formazan; plates were wrapped in foil and agitated on an orbital shaker for 1 h. Absorbance was read at 595 nm with a microplate reader (AMP Platos R 496, AMP Diagnostics, Austria). Cell viability was expressed as a percentage of untreated controls.

2.7. Propidium-iodide (PI) flow-cytometry assay

Following a 24 h exposure to each extract (100 μL per well), cultures were washed with PBS and detached with 30 μL trypsin-EDTA. Once cells rounded up, 50 μL PBS and 20 μL DMEM were added to quench trypsin, and suspensions were transferred to labelled 1.5 mL tubes. Cells were pelleted (5 min, 1500 rpm) and re-suspended in 500 μL PBS containing 1 μg mL^{-1} PI (1:10 stock dilution). After 15 min in the dark, samples were analyzed on a FACSCanto II cytometer (BD Biosciences, USA), acquiring 10 000 events per sample. PI-positive cells were quantified to determine the proportion of apoptotic/necrotic cells relative to total events.

2.8. Statistical analysis

Normality and homoscedasticity were verified (Shapiro–Wilk, Levene). All inferential tests were run at $\alpha = 0.05$ (OriginPro 2023, OriginLab Corp, USA). Kinetics data included a one-way ANOVA followed by Tukey post-hoc ($\alpha = 0.05$) compared DC_{max}, Rp_{max} and $t_{0.5}$ among formulations; while cytotoxicity – two-way ANOVA (*factor 1*: material; *factor 2*: polymerization state) with Tukey post-hoc analyzed MTT and PI data.

Table 1
Composition of commercial and experimental adhesives (wt%).

Category	Reagent/product	Supplier (city, country)	Notes
Monomers	Bis-GMA, UDMA, TEGDMA	Sigma-Aldrich (St Louis, USA)	≥98 % purity Bis-GMA Lot H13504543 UDMA Lot 72869864 TEGDMA Lot 0319250
	HEMA	Tokyo Chemical Industry (Tokyo, Japan)	≥99 % purity Lot SEPDB-KC
	G-IEMA dendrimer[b]	Synthesized in-house	G(2) poly(urethane-urea) core with eight methacrylate termini; protocol of Vasconcelos e Cruz et al. (2019) [17]
Functional monomer	10-MDP	DMHealthcare (San Diego, USA)	95 % purity Lot P01354
Photoinitiator system	Camphorquinone (CQ) & ethyl-4-dimethyl-aminobenzoate (BDA)	Sigma-Aldrich (St. Louis, USA)	0.4 mol % CQ: 0.8 mol % BDA in all formulations
Solvents	Ethanol (ACS) & ultrapure water (18 MΩ cm)	Carlo Erba (Milan, Italy)	–
Commercial controls	Scotchbond Universal (SBU)	3M ESPE (St. Louis, USA)	Universal adhesive [a]Composition: Bis-GMA (25–35 %) HEMA (15–25 %), 10-MDP (<20 %), Polyalkenoic acid copolymer (1–5 %), silane (7–13 %), camphorquinone (<2 %) water (5–15 %), ethanol (5–15 %)
	Futurabond M+ (FUT)	VOCO Gmbh (Cuxhaven, Germany)	Universal adhesive [a]Composition: Bis-GMA (10–25 %), HEMA (10–25 %), Acidic adhesive monomer (2.5–5 %), Ethanol (10–25 %)

[a] Composition derived from information supplied by the manufacturers, and the safety data sheets.
[b] Protocol is described in [17].

Table 2
Composition of commercial and experimental adhesives (wt%).

Component	SBU[a1]	FUT[a1]	EXP-BIS	EXP-GI
Bis-GMA	25–35 %	10–25 %	25	–
G-IEMA	–	–	–	25
UDMA	–	2.5–5 %	15	15
TEGDMA	N/A%	–	10	10
HEMA	15–25 %	10–25 %	10	10
10-MDP	<20 %	2.5–5 %	10	10
Other monomers	Polyalkenoic acid copolymer (1–5 %)	Methacrylate functionalized polyacid (N/A%)	–	–
Solvent (EtOH/H_2O)	5-15/5-15	10-25/N/A%	18-28/10-15	18-28/10-15
Initiator system	CQ-based	CQ-based	CQ/BDA	

[a] 1 Based on information supplied by the manufacturer.

3. Results

3.1. Homopolymers

3.1.1. Polymerization kinetics of homopolymers

Results for DC_{max}, Rp_{max} and $t_{0.5}$ are summarized in Fig. 2.

One-way ANOVA showed no difference in DC_{max} among monomers ($F = 1.6$, $p = 0.24$), indicating that, given sufficient time, each network achieved a comparable double-bond conversion. By contrast, Rp_{max} differed significantly ($F = 66.7$, $p < 0.0001$). Tukey post-hoc tests indicated UDMA > TEGDMA ≈ G-IEMA > HEMA, with Bis-GMA among the slowest: UDMA exceeded Bis-GMA, HEMA, G-IEMA, and TEGDMA (all $p < 0.001$); Bis-GMA exhibited the slowest rate, significantly lower than UDMA, TEGDMA, and G-IEMA ($p \leq 0.028$); G-IEMA matched TEGDMA and exceeded HEMA ($p < 0.01$). The half-time t0.5 did not differ among monomers ($F = 2.2$, $p = 0.15$), underscoring that variations in early propagation kinetics did not translate into differences in the time required to reach 50 % of DC_{max}.

Results for the instantaneous polymerization-rate profiles are summarized in Fig. 3. UDMA displayed a short induction period and the highest, sharpest peak reaching 6.6 % s^{-1} at ≈16–17 s before rapidly decaying. G-IEMA and TEGDMA showed intermediate maxima (~2–3 % s^{-1}); G-IEMA peaked earlier (≈16–20 s) with a shoulder, whereas TEGDMA was delayed and broader (≈21–24 s). HEMA and Bis-GMA exhibited low-amplitude, broad plateaus around ~1 % s^{-1}, with Bis-GMA the lowest overall.

3.1.2. MTT-assay and PI-flow cytometry of neat monomers

Results are summarized in Table 3. Two-way ANOVA detected main effects of monomer and polymerization treatment for both outcomes – metabolic activity and apoptosis, with significant interactions (MTT: $p = 0.003$; PI: $p = 0.002$; observed power >0.90).

MTT (metabolic activity): In uncured extracts, TEGDMA showed the highest activity, exceeding all other monomers ($p < 0.001$), while Bis-GMA was lowest and below HEMA ($p = 0.009$); no other uncured pairwise differences were detected. After polymerization, TEGDMA and HEMA again yielded the highest MTT values, each greater than G-IEMA, Bis-GMA, and UDMA ($p < 0.001$) and not different from each other. Within-monomer comparisons showed that only UDMA decreased upon curing ($p = 0.037$); other monomers were unaffected.

PI (apoptosis): In uncured extracts, Bis-GMA induced the greatest apoptosis, exceeding all other monomers ($p < 0.001$). After polymerization, Bis-GMA and TEGDMA remained highest: each exceeded G-IEMA and UDMA ($p < 0.001$), and Bis-GMA also exceeded HEMA ($p = 0.013$). Polymerization increased PI only for TEGDMA ($p < 0.001$); HEMA trended higher ($p = 0.052$); Bis-GMA, G-IEMA, and UDMA showed no change.

3.2. Commercial vs. experimental adhesives

3.2.1. Polymerization kinetics of commercial vs. experimental adhesives

Results for DC_{max}, Rp_{max}, and $t_{0.5}$ across the four adhesives are summarized in Fig. 4. One-way ANOVA showed no differences among Scotchbond Universal, Futurabond M+, EXP-BIS, and EXP-GI for DC_{max} ($F = 3.6$, $p = 0.06$), Rp_{max} ($F = 0.19$, $p = 0.89$), or $t_{0.5}$ ($F = 1.56$, $p = 0.27$).

3.2.2. MTT-assay and PI-flow cytometry of commercial vs. experimental adhesives

Results are summarized in Table 4. For MTT, two-way ANOVA found no interaction between adhesive and treatment ($p = 0.959$) and no main effect of polymerization ($p = 0.812$), but a main effect of adhesive ($p < 0.001$). Normalized to the 100 % control, all three test adhesives, EXP-GI, Scotchbond Universal, and Futurabond M+, reduced mitochondrial activity, with the control remaining statistically higher than every adhesive in both treatment states. Pairwise comparison revealed a single

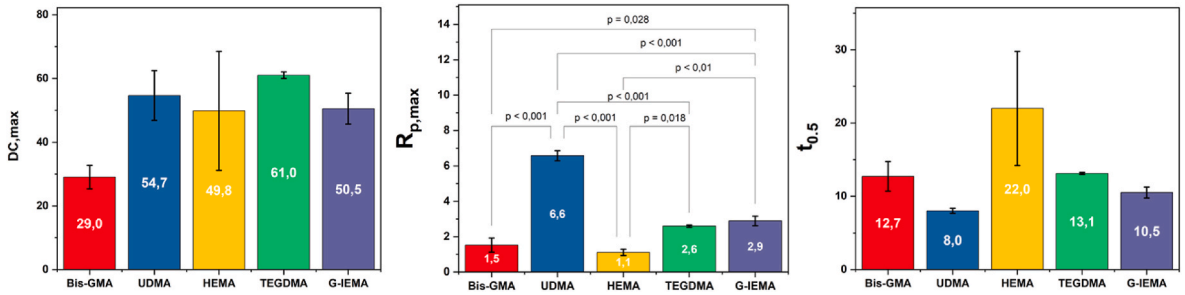

Fig. 2. Kinetic parameters of the five neat monomers. From left to right, panels show final degree of conversion (DC_{max}), maximum polymerization rate (Rp_{max}) and half-time to conversion ($t_{0.5}$). Columns represent the mean of three replicates ± standard error. Horizontal connectors with *p*-values identify pairwise differences detected by Tukey's post-hoc test (α = 0.05).

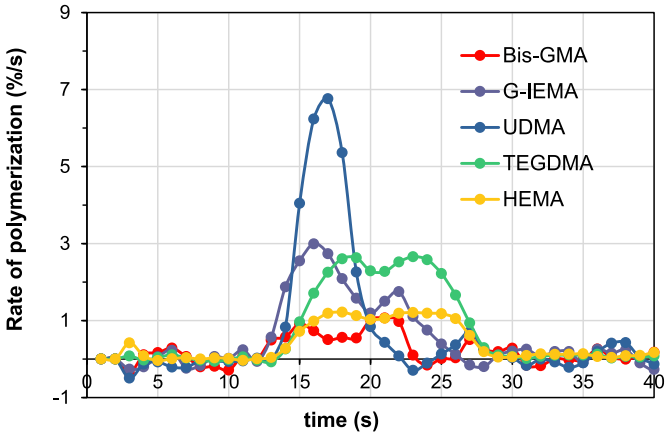

Fig. 3. Rate of polymerization (Rp, % s^{-1}) as a function of time for neat monomer homopolymerizations under identical photo-activation (0.4 mol% camphorquinone + 0.8 mol% ethyl-4-dimethylaminobenzoate; 900 mW/cm^2, 40 s; 22 ± 2 °C.

Table 3
Metabolic activity (through MTT) and apoptosis (PI) for neat monomers with error as standard error of the means.

Monomer		MTT (% activity ± SE)	PI (% apoptotic ± SE)
Bis-GMA	Uncured	24 ± 2.4	35 ± 2.6
	Cured	19 ± 2.5	40 ± 3.6
G-IEMA	Uncured	29 ± 2.2	21 ± 2.8
	Cured	29 ± 2.3	19 ± 2.2
UDMA	Uncured	31 ± 3.4	19 ± 2.8
	Cured	21 ± 2.2	15 ± 2.2
TEGDMA	Uncured	61 ± 4.6	17 ± 1.8
	Cured	60 ± 3.7	35 ± 4.1
HEMA	Uncured	40 ± 4.3	19 ± 2.2
	Cured	56 ± 4.5	27 ± 3.8

difference within the adhesive set: Futurabond M+ supported slightly higher metabolic activity than Scotchbond ($p = 0.007$); EXP-GI was indistinguishable from both commercial references.

For PI, the adhesive × treatment interaction was significant ($p = 0.019$). All adhesives exceeded the control ($p < 0.001$). Among uncured extracts, Futurabond M+ induced more apoptosis than Scotchbond Universal ($p = 0.006$), with EXP-GI intermediate (n.s. vs both). Polymerization reduced PI for Futurabond M+ ($p < 0.001$) and modestly for EXP-GI ($p = 0.049$), with no effect for Scotchbond Universal. No other adhesive pair differed under either treatment.

4. Discussion

4.1. Importance of the study and justification

The drive to eliminate bisphenol-A derivatives from dental materials has gained urgency as increasingly sensitive analytical methods continue to detect Bis-GMA and its hydrolysis product BPA in salivary and pulpal fluids long after restoration placement [12]. These observations, together with escalating regulatory pressure in the EU and USA, underline a critical need for high-performance, BPA-free resin matrices, that have been pursued in recent research [22,23]. G-IEMA, a generation-2 aliphatic dendrimer terminated with eight methacrylate groups, was conceived to address this need. It is a monomer with a globular geometry that may lower viscosity, enhance molecular mobility, and can thus yield cross-linked networks without aromatic backbones. The present investigation builds on earlier bond strength, nanoleakage, and mechanical characterization studies [17–19], by coupling real-time cure kinetics with cytocompatibility, to elucidate whether G-IEMA does indeed have a benefit over traditional dimethacrylates typically used in resin matrices.

4.2. Polymerization kinetics

The first null hypothesis—that substituting Bis-GMA with G-IEMA would leave polymerization kinetics unchanged— was indeed possible to accept. EXP-GI matched Scotchbond Universal, Futurabond M+ and its Bis-GMA analogue EXP-BIS in what regards the polymerization kinetic parameters DC_{max}, Rp_{max} and $t_{0.5}$. The behaviour of Bis-GMA helps explain why the EXP-GI adhesive could match kinetics despite replacing the aromatic base monomer. Chemically, Bis-GMA is a high-molecular-weight, rigid, di-functional dimethacrylate whose phenolic OH groups engage in extensive hydrogen bonding, producing very high viscosity and early diffusion-control during cure [10]; replacing or masking those OH groups is known to drop viscosity sharply [24]. Because mobility collapses early, a substantial fraction of pendant methacrylate groups remain unreacted under clinically realistic exposures. Thus, the effective functionality is often just one methacrylate group, with network formation dominated by diffusion-controlled kinetics and limited cyclization in the stiff, Bis-GMA–rich matrices [24,25]. These structural liabilities propagate to formulation level. One-bottle/universal systems must juggle hydrophobic Bis-GMA/UDMA with hydrophilic HEMA and water/ethanol, and multiple studies show phase separation of Bis-GMA/HEMA copolymers in the presence of water and a reliance on HEMA to suppress phase splitting, at the cost of increased water sorption and hydrolytic vulnerability [26,27]. G-IEMA contrasts these results. It is a second-generation dendritic macromer bearing eight terminal methacrylate groups on an aliphatic core, providing multiple reactive termini within a compact, low-aromatic architecture that facilitates network percolation at lower radical concentrations. Such findings are interesting since dendrimers, owing to their steric bulk, are often

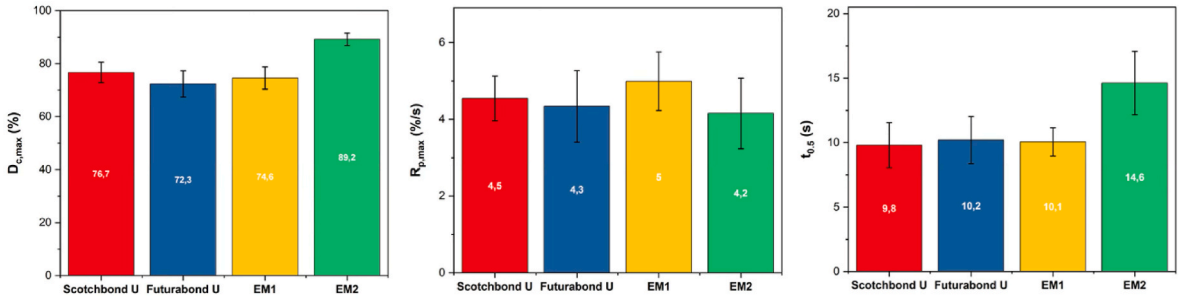

Fig. 4. Kinetic parameters of the two commercial adhesives (Scotchbond Universal, Futurabond Universal) and the two experimental formulations (EXP-BIS, EXP-GI). Bars display mean ± standard error for DC_{max}, Rp_{max} and $t_{0.5}$ ($n = 3$). One-way ANOVA followed by Tukey's test revealed no statistically significant differences among the four systems for any parameter.

Table 4
Metabolic activity (through MTT) and apoptosis (PI) for the commercial vs. experimental adhesives, with error as standard error of the means.

Adhesive	State	MTT (% activity ± SE)	PI (% apoptotic ± SE)
Futurabond M+	Uncured	56 ± 3.4	38 ± 3.3
	Cured	55 ± 3.9	26 ± 2.3
Scotchbond Universal	Uncured	42 ± 3.4	27 ± 1.6
	Cured	41 ± 4.6	28 ± 3.1
EXP-GI	Uncured	45 ± 3.7	30 ± 1.8
	Cured	49 ± 4.8	23 ± 2.1
Control	–	100	12 ± 0.9

assumed to impede monomer chain propagation. Instead, a reduction of macro-viscosity relative to the rigid aromatic backbone found in Bis-GMA was noted [16,28]. The homopolymer data reinforce this interpretation — G-IEMA polymerized over twice as fast as Bis-GMA and at a rate comparable to TEGDMA, traditionally employed as a low-viscosity diluent. Also, the numerically higher conversion of EXP-GI (≈89 %), although not significant, it is past the 80 % conversion plateau, which can be regarded as a practical ceiling for photopolymerizable aromatic dimethacrylates [29,30]. Formulation-wise, the lower macro-viscosity and high functionality of G-IEMA create room to reduce HEMA content (mitigating water uptake) while maintaining a single-phase mixture—an avenue aligned with contemporary reviews on composition–phase behaviour in universal adhesives and with our finding that a Bis-GMA-free matrix can deliver a conventional cure profile without a cytotoxicity penalty [31,32].

Under a thin-film, relatively high-irradiance protocol, the quantity of photons and overall mobility were not limiting, so Bis-GMA– and G-IEMA–based adhesives converged in DC_{max}, Rp_{max} and $t_{0.5}$. Indeed, when radiant exposure is ample and films are thin, many dimethacrylate matrices display similar surface-proximal curing behaviour [33]. As film thickness increases, the bottom layers receive less light due to absorption and scattering, and vitrification reduces mobility at depth—conditions under which monomer architecture and resin–filler refractive-index match are responsible for more strongly governing bottom-layer conversion [34]. These depth effects are best seen with spatially resolved methods (Raman/FTIR mapping), which can reveal differences invisible to surface-sensitive ATR-FTIR [35]. Protocol changes are likewise expected to reveal architectural advantages. Reducing radiant exposure, increasing the distance from the tip or using alternative photoinitiation (polywave LEDs; PO-based systems) may drive networks toward radical-flux and mobility limits where aliphatic, multi-functional methacrylate monomers should better sustain conversion than aromatic Bis-GMA matrices.

Over longer elution windows, differences may widen: as water sorption and network relaxation dominate, cumulative release becomes diffusion-controlled and tracks cross-link density and solubility, so network architecture (e.g., G-IEMA vs Bis-GMA) can then influence the amount and kinetics of leachables [36,37].

The high functional group density seen with the dendrimer should also favor tightly cross-linked nanodomains, yet its flexible urethane core can dissipate shrinkage stress more efficiently than the rigid aromatic spine seen in Bis-GMA [32]. This combination—high conversion with controlled stress—is exactly what finite-element models deem most critical for maintaining marginal integrity under thermo-mechanical cycling. While shrinkage stress was not measured here, our earlier tensile bond-strength and nanoleakage studies indirectly support the premise, EXP-GI showed equal immediate μTBS but significantly lower nanoleakage after thermocycling compared with its Bis-GMA analogue. Limited light transmission through Bis-GMA–rich matrices is also a documented problem. First, the aromatic rings absorb photons in the 385–420 nm tail of most dental LED units; second, the pronounced refractive-index mismatch between Bis-GMA (n ~ 1.55) and silanized barium-glass filler (n ~ 1.48) amplifies Rayleigh scattering. In combination, these mechanisms reduce delivered blue irradiance by a factor of two to three at just 1 mm depth, as documented by Price et al. [34] and by Shortall, Palin and Burtscher [38]. Replacing Bis-GMA with the aliphatic dendrimer G-IEMA should mitigate both losses: Lorentz–Lorenz calculations, based on the molar polarizability and measured density of neat G-IEMA, predict a refractive index close to 1.50. This value, if confirmed experimentally, would reduce the resin–filler refractive-index mismatch (Δn) from ~0.07 in Bis-GMA-rich matrices to ~0.02, a ten-fold drop in Rayleigh scattering intensity. Altogether, such data indicate that G-IEMA is a comparable substitute to Bis-GMA but may even enhance the photoreactivity of a universal adhesive, offering formulators a route to higher conversion without increasing diluent content.

4.3. Biocompatibility assays

The homopolymer of Bis-GMA consistently ranked as the most cytotoxic dimethacrylate, while TEGDMA shows deceptively high metabolic activity yet triggers substantial apoptosis once organized into a polymer network. The poor performance seen in Bis-GMA is generally attributed to its lipophilicity (log P ~ 4.4) and its ability to enter cells and deplete glutathione, leading to ROS accumulation and DNA damage [39]. By contrast, TEGDMA is hydrophilic (log P ~ 1.4) and penetrates cells quickly; polymerization converts a fraction of TEGDMA into short, water-soluble oligomers that leach more readily than the parent monomer [40], explaining the rise in PI-labelled apoptosis that was observed after curing.

The homopolymer of G-IEMA was equivalent to UDMA in the low-toxicity tier for both metabolic and apoptotic endpoints. Like UDMA, G-IEMA lacks aromatic rings and carries urethane linkages, features associated with a lower lipophilicity and reduced membrane disruption [41]. Its high molecular weight (~1.5 kDa) may further limit passive diffusion across the cell membrane, reducing intracellular exposure.

For adhesive eluates, metabolic activity differed among materials but

not between polymerized and uncured states, whereas apoptosis did respond to polymerization in two of the three adhesives. It is likely that formulation chemistry governs this. Futurabond and EXP-GI both use ethanolic predominant solvents and contain 10-MDP as the main acidic monomer, whereas Scotchbond relies on water/ethanol/HEMA and a proprietary polyalkenoic acid copolymer, other than 10-MDP. Post-cure reductions in apoptosis for Futurabond and EXP-GI suggest that higher final conversion (82–89 %) immobilizes a larger fraction of residual monomer and initiator fragments, leaving fewer leachables. Regarding Scotchbond, its static PI values, despite curing, may reflect its lower DC (~75 %) and the presence of hydrophilic copolymers that continue to leach even after polymerization, a phenomenon already noted in literature-reported findings [42].

In this study, monomers such as TEGDMA and HEMA, achieved a higher apoptotic percentage after curing, which may present as a counter-intuitive finding. This can be traced to chemical differences after polymerization. Light irradiation generates new, often more cytotoxic species. Camphorquinone and tertiary-amine co-initiators degrade into aldehydes and α-diketones; diphenyl-phosphine oxide or benzoyl-based initiators yield benzoyl and phosphinyl radicals that persist in the polymer matrix and have been linked to elevated reactive-oxygen production and apoptosis [43,44]. These photolytic fragments are absent from the non-polymerized extract.

Polymerization can also shift the polarity balance. TEGDMA and HEMA, for example, react to form short, hydrophilic oligomers that are far more water-soluble than their parent monomers; once formed, they diffuse out quickly and can reach higher effective concentrations in the culture medium, explaining why polymerized TEGDMA showed greater PI induction than its uncured form in these findings. Similar results have been documented for self-adhesive cements and universal adhesives where polymerized eluates became increasingly cytotoxic over time despite higher degree of conversion [45]. Finally, micro-radicals trapped in the freshly cured network can continue to generate low-level ROS during extraction, compounding oxidative stress in cell assays.

4.4. Limitations and recommendations for future research

First, the biological assays captured only a 24-h window of cellular response; delayed oxidative stress, inflammatory signalling and genotoxicity were not monitored and remain pertinent for future research. Second, a single radiant exposure (950 mW/cm^2, 15 s) and constant film thickness were tested; different light outputs and thicker layers are expected to shift both conversion and leachable profiles. Also, the eluates were analyzed as gross extracts without chemical speciation, so the particular photolysis products or unreacted monomers that may be driving cytotoxicity remain unidentified. It is also important to consider that the present in-vitro model used primary human pulp cells exclusively and that fibroblasts, macrophages and endothelial cells may respond differently. Future studies should also quantify leachables from G-IEMA-based adhesives over extended ageing in artificial saliva and under thermo-mechanical cycling to simulate the oral environment. Finally, exploration of higher-generation dendrimers or partially fluorinated analogues may further enhance network density and solvent resistance, pushing universal adhesives toward improved performance and minimal biological footprint.

It is important to mention that the translational case for G-IEMA is timely given the EU's trajectory. The re-evaluation in 2023 by the EFSA lowered the tolerable daily intake for BPA to 0.2 ng/kg bw/day [46], prompting the European Commission to adopt Commission Regulation (EU) 2024/3190 in December 2024, which bans BPA (and certain other bisphenols) in food-contact materials and entered into force on 20 January 2025 [47]. This proves sustained regulatory pressure to exit BPA-rich chemistries. In this context, our finding that a BPA-free, dendrimer-based adhesive matches market comparators for cure kinetics and acute cytocompatibility underscores a potential practical compliance advantage. Manufacturers can remove Bis-GMA without sacrificing handling or performance, aligning product portfolios with emerging EU restrictions. To convert these laboratory assays into future industrial material development, the next assays should include long-term leachables profiling under thermo-hydrolytic/thermocycling stress (e.g., ISO-guided cycling and water storage) coupled to time-resolved LC-MS/MS, since composites and adhesives can continue releasing trace monomers and by-products for months to a year under dynamic extraction. Finally, because dendritic architecture is a design variable, testing higher-generation dendrimers (greater functionality at similar viscosity) is warranted, a direction already highlighted in recent high-impact reviews of BPA-free adhesive monomers that specifically discuss G-IEMA as a promising platform for durable, hydrolytically stable interfaces [32].

5. Conclusions

Replacing Bis-GMA with the dendrimeric macromer G-IEMA yielded a universal adhesive that matched market comparators in degree of conversion, peak rate, and half-time to cure, and showed no penalty in acute cytocompatibility. As neat monomer, G-IEMA ranked among the least cytotoxic in primary pulp cells, contrasting with the unfavorable profile of Bis-GMA. These findings indicate that dendritic architecture can deliver the crosslinking capacity historically sought from Bis-GMA without importing its biological liabilities, thereby advancing a credible BPA-free path for adhesive design.

Practically, G-IEMA preserves the curing headroom needed to rebalance matrix composition—e.g., lowering HEMA or reactive diluents, tuning solvent, or increasing functional monomers, without sacrificing cure performance. Its profile also suggests translational potential beyond single-bottle adhesives, including resin cements, flowables, and low-shrinkage restorative matrices where high conversion under constrained light doses is critical. This dendrimer therefore represents a viable, BPA-free platform for next-generation restorative materials.

CRediT authorship contribution statement

Diogo Monteiro: Writing – original draft, Methodology, Investigation, Conceptualization. **Margot Barbier:** Writing – original draft, Investigation, Conceptualization. **António HS Delgado:** Writing – review & editing, Writing – original draft, Supervision, Methodology, Data curation, Conceptualization. **Luísa Gonçalves:** Writing – original draft, Supervision, Investigation, Data curation. **Miguel Chaves-Ferreira:** Supervision, Methodology, Investigation. **Joana Vasconcelos e Cruz:** Writing – original draft, Methodology, Investigation, Conceptualization. **Mário Polido:** Supervision, Formal analysis, Data curation.

Declaration of competing interest

The authors declare that they have no known competing financial interests or personal relationships that could have appeared to influence the work reported in this paper.

Acknowledgements

None.

Data availability

Data will be made available on request.

References

[1] Perdigão J, Swift Jr EJ. Universal adhesives. J Esthetic Restor Dent 2015;27(6):331–4.
[2] Nagarkar S, Theis-Mahon N, Perdigão J. Universal dental adhesives: current status, laboratory testing, and clinical performance. J Biomed Mater Res B Appl Biomater 2019;107(6):2121–31.

[3] Ismail IH, Razak NAA, Ramzi NDM, et al. Microtensile bond strength of total-etch and self-etch universal adhesives containing 10-MDP: a systematic review. J Dent 2022;10:12–24.
[4] Perdigão J, Sezinando A.
[5] Araújo-Neto VG, Moreira MM, Ñaupari-Villasante R, et al. Nanofiller particles and bonding durability, water sorption, and solubility of universal adhesives. Operat Dent 2021;46(6):690–7.
[6] Sai K, Shimamura Y, Takamizawa T, et al. Influence of degradation conditions on dentin bonding durability of three universal adhesives. J Dent 2016;54:56–61.
[7] Yoshioka M, Yoshida Y, Inoue S, et al. Adhesion/decalcification mechanisms of acid interactions with human hard tissues. J Biomed Mater Res 2002;59(1):56–62.
[8] Van Meerbeek B, Yoshihara K, Van Landuyt K, et al. From buonocore's pioneering acid-etch technique to self-adhering restoratives. A status perspective of rapidly advancing dental adhesive technology. J Adhesive Dent 2020;22(1):7–34.
[9] Yoshihara K, Yoshida Y, Hayakawa S, et al. Nanolayering of phosphoric acid ester monomer on enamel and dentin. Acta Biomater 2011;7(8):3187–95.
[10] Barszczewska-Rybarek IM. A guide through the dental dimethacrylate polymer network structural characterization and interpretation of physico-mechanical properties. Materials 2019;12(24):4057.
[11] Durner J, Schrickel K, Watts DC, et al. Direct and indirect eluates from bulk fill resin-based-composites. Dent Mater 2022;38(3):489–507.
[12] De Angelis F, Sarteur N, Buonvivere M, et al. Meta-analytical analysis on components released from resin-based dental materials. Clin Oral Invest 2022;26 (10):6015–41.
[13] Drozdz K, Wysokinski D, Krupa R, et al. Bisphenol A-glycidyl methacrylate induces a broad spectrum of DNA damage in human lymphocytes. Arch Toxicol 2011;85 (11):1453–61.
[14] Vom Saal FS, Antoniou M, Belcher SM, et al. The conflict between regulatory agencies over the 20,000-fold lowering of the tolerable daily intake (TDI) for bisphenol A (BPA) by the European Food Safety Authority (EFSA). Environ Health Perspect 2024;132(4):45001.
[15] Tichy A, Srolerova T, Schwendicke F. Release of bisphenol A from dental materials: risks and future perspectives. J Dent Res 2025;104(10):1051–60. https://doi.org/10.1177/00220345251337728.
[16] Yu B, Liu F, He J. Preparation of low shrinkage methacrylate-based resin system without Bisphenol A structure by using a synthesized dendritic macromer (G-IEMA). J Mech Behav Biomed Mater 2014;35:1–8.
[17] Vasconcelos e Cruz J, Brito J, Polido M, et al. A new experimental adhesive system containing G-IEMA – physicochemical properties. J Adhes Sci Technol 2019;33(4): 418–32.
[18] Vasconcelos E, Cruz J, Polido M, Brito J, et al. Dentin bonding and SEM analysis of a new experimental universal adhesive system containing a dendrimer. Polymers 2020;12(2):461.
[19] Vasconcelos ECruz J, Delgado AHS, Félix S, et al. Improving properties of an experimental universal adhesive by adding a multifunctional dendrimer (G-IEMA): bond strength and nanoleakage evaluation. Polymers 2022;14(7):1462.
[20] Delgado AHS, Young AM. Methacrylate peak determination and selection recommendations using ATR-FTIR to investigate polymerisation of dental methacrylate mixtures. PLoS One 2021;16(6):e0252999.
[21] Vasconcelos e Cruz J. Propriedades físico-químicas, mecânicas e citotóxicas de um novo sistema adesivo dentário contendo um dendrímero. Universidade do Porto; 2020. Instituto Ciências Biomedicas Abel Salazar [cited 2025 Sept 6]. Available from: https://hdl.handle.net/10216/129420.
[22] Sun Y, Zhou Z, Jiang H, et al. Preparation and evaluation of novel bio-based Bis-GMA-free dental composites with low estrogenic activity. Dent Mater 2022;38(2): 281–93.
[23] Yoshinaga K, Yoshihara K, Yoshida Y. Development of new diacrylate monomers as substitutes for Bis-GMA and UDMA. Dent Mater 2021;37(6):e391–8.
[24] Lovell LG, Stansbury JW, Syrpes DC, et al. Effects of composition and reactivity on the reaction kinetics of dimethacrylate/dimethacrylate copolymerizations. Macromolecules 1999;32(12):3913–21.
[25] Elliott JE, Lovell LG, Bowman CN. Primary cyclization in the polymerization of bis-GMA and TEGDMA: a modeling approach to understanding the cure of dental resins. Dent Mater 2001;17(3):221–9.
[26] Ye Q, Wang Y, Spencer P. Nanophase separation of polymers exposed to simulated bonding conditions. J Biomed Mater Res B Appl Biomater 2009;88(2):339–48.
[27] Abedin F, Ye Q, Parthasarathy R, et al. Polymerization behavior of hydrophilic-rich phase of dentin adhesive. J Dent Res 2015;94(3):500–7.
[28] Yu B, Liu F, He J, et al. Preparation of bis-GMA-free dental restorative composites with dendritic macromer (G-IEMA). Adv Polym Technol 2015;34(4) [Internet].
[29] Stansbury JW, Dickens SH. Determination of double bond conversion in dental resins by near infrared spectroscopy. Dent Mater 2001;17(1):71–9.
[30] Sideridou I, Tserki V, Papanastasiou G. Effect of chemical structure on degree of conversion in light-cured dimethacrylate-based dental resins. Biomaterials 2002;23 (8):1819–29.
[31] Dressano D, Salvador MV, Oliveira MT, et al. Chemistry of novel and contemporary resin-based dental adhesives. J Mech Behav Biomed Mater 2020;110(103875): 103875.
[32] Cadenaro M, Josic U, Maravić T, et al. Progress in dental adhesive materials. J Dent Res 2023;102(3):254–62.
[33] Price RB, Ferracane JL, Shortall AC. Light-curing units: a review of what we need to know: a review of what we need to know. J Dent Res 2015;94(9):1179–86.
[34] Price RB, Murphy DG, Dérand T. Light energy transmission through cured resin composite and human dentin. Quintessence Int 2000;31(9):659–67.
[35] Gatin E, Iordache S-M, Matei E, et al. Raman spectroscopy as spectral tool for assessing the degree of conversion after curing of two resin-based materials used in restorative dentistry. Diagnostics 2022;12(8):1993.
[36] Van Landuyt KL, Nawrot T, Geebelen B, et al. How much do resin-based dental materials release? A meta-analytical approach. Dent Mater 2011;27(8):723–47.
[37] Malacarne J, Carvalho RM, de Goes MF, et al. Water sorption/solubility of dental adhesive resins. Dent Mater 2006;22(10):973–80.
[38] Shortall AC, Palin WM, Burtscher P. Refractive index mismatch and monomer reactivity influence composite curing depth. J Dent Res 2008;87(1):84–8.
[39] Reichl F-X, Simon S, Esters M, et al. Cytotoxicity of dental composite (co) monomers and the amalgam component Hg(2+) in human gingival fibroblasts. Arch Toxicol 2006;80(8):465–72.
[40] Mikulás K, Komlódi T, Földes A, et al. Bioenergetic impairment of triethylene glycol dimethacrylate- (TEGDMA-) treated dental pulp stem cells (DPSCs) and isolated brain mitochondria are amended by redox compound methylene blue. Materials 2020;13(16):3472.
[41] Bakopoulou A, Papadopoulos T, Garefis P. Molecular toxicology of substances released from resin-based dental restorative materials. Int J Mol Sci 2009;10(9): 3861–99.
[42] Massaro H, Zambelli LFA, Britto AA de, et al. Solvent and HEMA increase adhesive toxicity and cytokine release from dental pulp cells. Materials 2019;12(17):2750.
[43] de Melo Soares V, Cândido dos Reis A, Lima da Costa Valente M. The influence of 2,4,6-trimethylbenzoyldiphenylphosphine oxide on the toxicity of dental resins: a systematic review of in vitro studies. Int J Adhesion Adhes 2025;138(103922): 103922.
[44] Kowalska A, Sokolowski J, Bociong K. The photoinitiators used in resin based dental composite-A review and future perspectives. Polymers 2021;13(3):470.
[45] Cangul S, Adiguzel O, Tekin S. Comparison of cytotoxicity of four different adhesive materials before and after polymerisation. Oral Health Prev Dent 2020;18 (1):43–52.
[46] Ramírez V, Merkel S, Tietz T, et al. Risk assessment of food contact materials. EFSA J 2023;21(Suppl 1):e211015.
[47] European Comission (EU). EU prohibition on the use and trade of Bisphenol A from 20 January 2025 [Internet][cited 2025 Sept 17]. Available from: https://trade.ec.europa.eu/access-to-markets/en/news/eu-prohibition-use-and-trade-bisphenol-20-january-2025; 2025.